1. INTRODUCTION

1.1 SURVIVAL IN THE MACROPHAGE

M. tuberculosis (Mtb) has affected humanity throughout history. The World Health Organization (WHO) has estimated that one third of the world's population is infected with Mtb, with about eight million new cases diagnosed annually [1]. Not much is known about the physiological and immunological responses of the host to infection and the biology of Mtb in its natural setting [2].

Mycobacteria survive within macrophages by inhibiting the maturation of phagosomes into fully bactericidal phagolysosomes [3]. Electron microscopy studies of *M. avium* infection in mice deficient in Nramp1, show that Nramp is recruited to the membrane of *M. avium* containing phagosomes in wild type mice, causing bacteriostasis, increased bacterial damage, increased acidification and increased fusion to lysosomes when compared to Nramp$I^{-/-}$ phagosomes [4]. A simplified explanation for this could be provided with the hypothesis that, inhibition of phagosome maturation of mycobacteria requires a metal dependant process that can be antagonized by NrampI mediated metal efflux from the phagosomal lumen. The presence in culture filtrates of proteins e.g. ESAT-6, SodA [5], GlnA [6] and KatG suggest the existence of protein secretion systems that operate in *Mycobacterium tuberculosis* (Mtb) [7,8]. Identification of the secreted metalloproteins of Mtb would open a way to study the corelation between the existence of the metal transporting pumps and pathogen survival. The secreted components like the SODs that are involved in prevention of ROS (Reactive Oxygen Species) and RNS (Reactive Nitrogen Species) stress to the Mycobacteria in the phagosome have an active metal centre. It is

hence relevant to consider metals as one of the most important components of intra-phagosomal survival by Mtb.

1.2 REACTIVE OXYGEN SPECIES AND REACTIVE NITROGEN SPECIES

ROS and RNS are defense mechanisms generated by the host macrophage on encounter with a pathogen. Recent studies involving mice deficient in the respiratory burst oxidase or inducible nitric oxide synthase have shown the importance of reactive oxygen and nitrogen intermediates in mammalian immunity [9]. The term "RNS" refers to oxidation states of the nitrogenous products of Nitric Oxide Synthases (NOS), they range from nitric oxide (•NO) to nitrate (NO_3^-). The most common RNS encountered in physiological environments are NO, $\bullet NO_2$, NO_2^-, N_2O_3, N_2O_4, *S*-nitrosothiols, peroxynitrite ($OONO^-$), and dinitrosyl-iron complexes [10]. The term "ROS" refers to intermediate reduced products of O_2 en route to water, superoxide ($O_2^{\bullet -}$) hydrogen peroxide (H_2O_2) and hydroxyl radical (OH•) along with reactive products of these with halides and amines [11,12].

Antioxidant defense systems have evolved to protect cells against ROS damage. They include the enzymes glutathione peroxidase, glutathione reductase, copper and zinc-dependent superoxide dismutase (Cu-ZnSOD), catalase and manganese-dependent superoxide dismutase (MnSOD)(Fig. 1).

Mtb exports several proteins into the phagosome. The functions of these proteins are related to cellular homeostasis like cell wall synthesis and energy generation. Others are directly associated with detoxification of ROS and RNS in noxious environments of the phagosome [13,14]. It has been

established that protein export pathways play an important role in bacterial pathogenesis. Most of the bacterial virulence factors are exported proteins and systems responsible for their export are critical to virulence [15]. The Sec-dependant protein export pathway is conserved throughout all bacteria and is responsible for the translocation of precursor proteins containing classical amino terminal signal sequences across the cytoplasmic membrane. Mycobacteria possess multiple *secA* genes (*secA1*, *secA2*) in their genomes [16]. These exported proteins are one of the first molecules to interact with the host and protein export is critical to virulence. SecA2 is known to be required for the optimal secretion of superoxide dismutase (SodA) and catalase-peroxidase (KatG). Both these proteins function to detoxify ROS [16]. Many of these enzymes are metalloproteins. Some are loaded in the cytoplasm with the metal and then secreted in the folded state through the TAT system. Others however are secreted unfolded via the Sec pathway and they then acquire their cofactors in the periplasm [17]. Heavy metal sensing in the cell is far from being properly understood [18]. In recent years it has been observed that there is almost no free metal present in a living cell and the metals are handed down from one protein to another through chaperones and efflux systems [19,20].

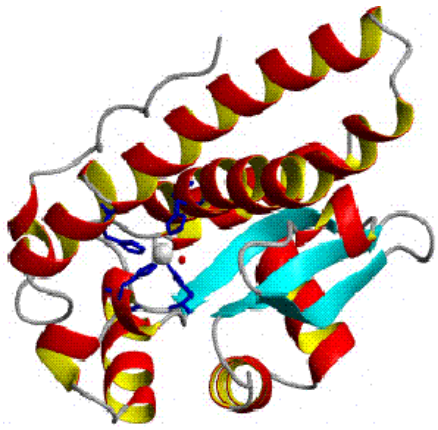

Fig. 1: Structure of the monomeric unit of human superoxide dismutase 2 (SOD2), showing the Zinc cofactor in the centre.

1.3 P-TYPE ATPASES

The regulation of metal ion concentrations is central to the physiology of all organisms. Mtb encodes 28 putative metal ion transporters based on sequence homology analysis [21]. Cation transporters in Mtb represent 24% of all encoded transporter sequences. This repertoire of transporters confers the versatility required for adaptation to intracellular and extracellular niches [22]. Out of these, 12 are active transporters or P-type ATPases. Here ATP hydrolysis provides the energy for cation transport across the membrane. P-type ATPases; transport a variety of monovalent and divalent metals across membranes using the energy of hydrolysis of the terminal phosphate bond of ATP. They are thought to appear in early evolution and are key proteins in the maintenance of metal homeostasis in all organisms.

Analysis of P-type ATPase sequences in Mtb have shown that some of them have 8 TM helices [23,24], evidence has also been found of ATPases with 6, 7 and 10 TM helices [25-28].

In the ATPases with 8 TM helices, the conserved residues in TMs H6, H7 and H8 form the Trans Membrane – Metal Binding Domain (TM-MBD) and provide the signature sequences that predict the metal sensitivity of the P-type ATPases [29 30]. The large loop between TMs H6 and H7 represents the cytoplasmic loop responsible for ATP binding and hydrolysis. This loop is called the ATP Binding Domain (ATP-BD). This is made up of the nucleotide (N) binding and phosphorylation (P) domains (Fig. 2) [31]. A "hinge" region separates the two domains. The smaller cytoplasmic loop between TM H4 and H5 forms the actuator (A) domain [32].

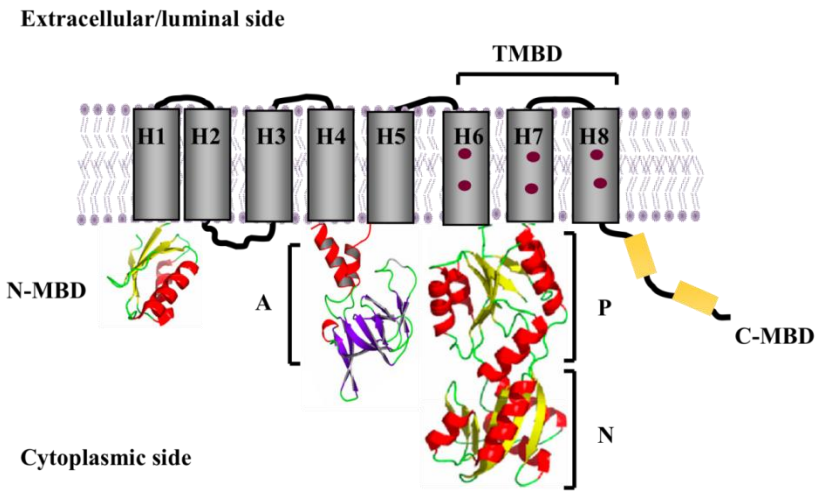

Fig. 2: A schematic representation of the membrane topology of a P-type ATPase. Transmembrane helices, H1-H8, are indicated. The relative locations and structure of *Archaeoglobus fulgidus* CopA actuator (A) domain and phosphorylation (P) and nucleotide (N) domains [31,32]are shown. To represent one of the repeats present in the N-terminus the human Menkes disease protein (MNK) fifth N-terminal metal binding domain (N-MBD)[33] is depicted. The conserved amino acids in H6, H7 and H8 forming the transmembrane metal binding domain (TM-MBD) are symbolized by red dots. The C-terminal metal binding domains (C-MBDs) with likely diverse structures are represented by yellow rectangles

Active transport of the metal by P-type ATPases follows the E1-E2 Albers-Post model, alternating the affinities of intracellular metal binding sites from high (E1) to low (E2) (Fig. 3) [34]. In the E1 state the ATPase has a high affinity for metal and the TM-MBDs are accessible from the cytoplasmic side. In contrast, an enzyme in the E2 state has low affinity for the metal and in this conformation the metal binding site faces the opposite side of the membrane. According to this model, enzyme in E1 state is phosphorylated by Mg-ATP (μM) with metal ion binding to the TM-MBDs from the cytoplasmic side (E1.ATP.nM). The phosphorylation occurs with the transfer of the terminal phosphate of ATP to a conserved Asp residue located in the P-domain followed by the subsequent release of ADP ($E1.P.xM^{+n}$). This phosphorylation causes occlusion of the bound metal ion at the TM-MBDs. The enzyme is unstable in the E1.P state and converts rapidly to the E2.P state. This transition leads to the release of the metal ions into the

extracellular/luminal compartment. Finally, dephosphorylation takes place and the enzyme returns to the dephosphorylated state and metal is freed from E2. The enzyme then returns to the E1 conformation on ATP (mM) binding to E2.

Biochemical studies with eukaryote, prokaryote and archeal P_{1B}-type ATPases have provided evidence for individual steps of the catalytic mechanism. ATPase activity, phosphorylation, dephosphorylation and metal transport studies have been carried out with isolated or membrane preparations of Cu^{+}- and Zn^{2+}-ATPases [35 36 37 38 39 40].

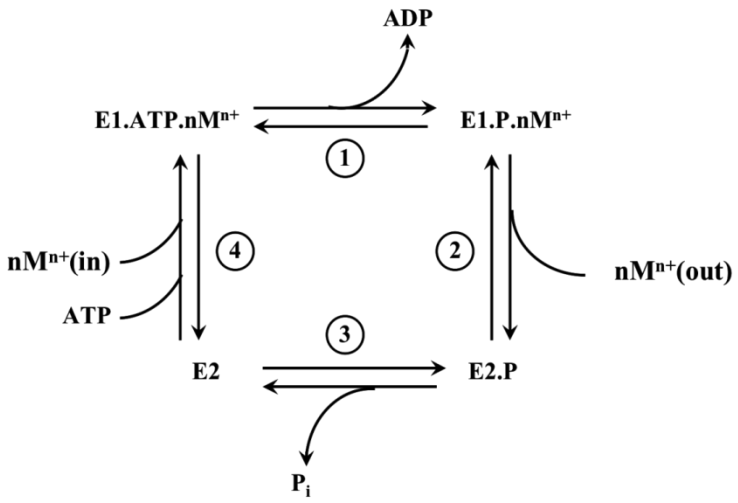

Fig. 3: Catalytic Mechanism of P1B-type ATPases. E1 and E2 represent the different conformations of the enzyme. M+n represent the different metals that are transported by P1B-type ATPases. n indicates the uncertainty on the stoichiometry of the metal transport. M+n (in) represents the cytoplasmic and M+n (out) represents the extracellular or luminal localization of the transported metal.

Transport experiments show that P_{1B}-type ATPases drive metal efflux from the cytoplasm [35] [36] [37] [41] [40]. This agrees with a mechanism where the enzyme binds to ATP and the metal in the E1 state (TM-MBDs are open to the cytoplasmic site). Some earlier reports suggest that some Cu^{+}-ATPases might drive metal influx into the cytoplasm [42,43]. This would however require an alternative mechanism where the binding of another substrate would be required in the E1 state to trigger ATP hydrolysis and enzyme phosphorylation followed by subsequent conformational changes to allow metal influx. The direction of transport of metal by the Mtb ATPases has not yet been defined. We have addressed this issue for one of these ATPases through experiments using *E. coli* transformed with ctpC.

1.4 TRANSMEMBRANE METAL BINDING SITES AND CLASSIFICATION OF P-TYPE ATPASES

P-type ATPases transport a variety of ions against their concentration gradients using the energy they acquire from ATP hydrolysis in the cytoplasm. The Na, K ATPase, Sarcoplasmic Reticulum (SR) Calcium ATPase, yeast Proton ATPase and the Gastric H, K ATPase are all well studied examples of P-type ATPases [44] [45].

Type IA ATPases are found only in bacteria. Based on their primitive structure, they may be ancestral proteins. Type IB ATPases are found in bacteria, archaea and eukaryotes and are speculated to have evolved early in evolution. Type IIA and Type III ATPases are found in archaea, plants and fungi, but not in bacteria, and therefore must have evolved later. Type IV, type V (Fig. 4), type IIB and type IID are only found in eukaryotes and probably evolved after the split between archaea and eukaryote [24] [25].

Most of the P_{1B} ATPases contain a CPX signature sequence in the helix previous to the DKTGT sequence. The proline seems to be conserved in all P-type ATPases and has known to be important for metal binding and transport [29 24 26 27 46 28]. Mutations to this proline in some Cu^+ ATPases have yielded proteins that were deficient in ATPase activity. [36 47 48 49]

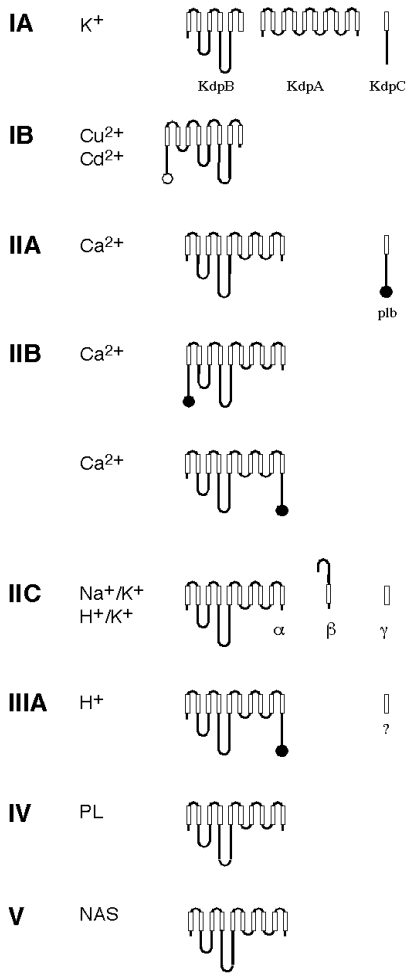

Fig. 4: Overview of the P-type ATPase Family: Families are designated by roman numerals on the left followed by the name of the transported ion. Boxes indicate transmembrane segments; Filled circles, inhibitory sequences; Open circles, heavy metal binding sites. Abbreviations are: PL, phospholipids; NAS, no assigned specificity; plb, phospholamban. The (subunit of type IIC ATPases so far has only been shown to be associated with Na^+/K^+-ATPase isozymes. It is uncertain whether association with a proteolipid is a general feature of type IIIA ATPases. This is indicated by a question mark.

P-type ATPases have several conserved segments that can be identified by multiple alignment [24]. These domains are situated in the helix preceding the DKTGT domain and the following two helices after the DKTGT domain. In P_{1B} ATPases the sequence CPC, CPH, SPC precedes the DKTGT sequence on TM 6 (Fig. 5). Besides this consensus, there are additional sequences on TM 7 and TM 8 that helps to sub classify these ATPases into P_{1B1}-P_{1B5}. [50 51 52 53 54 55]. The large cytoplasmic loops between these helices are believed to be involved in any possible communication with the chaperones in the cytoplasm that helps to ferry the metal across the plasma membrane. They are also known to be involved in communication with other parts of the protein for inducing conformational changes, ion binding and ATP hydrolysis [29].

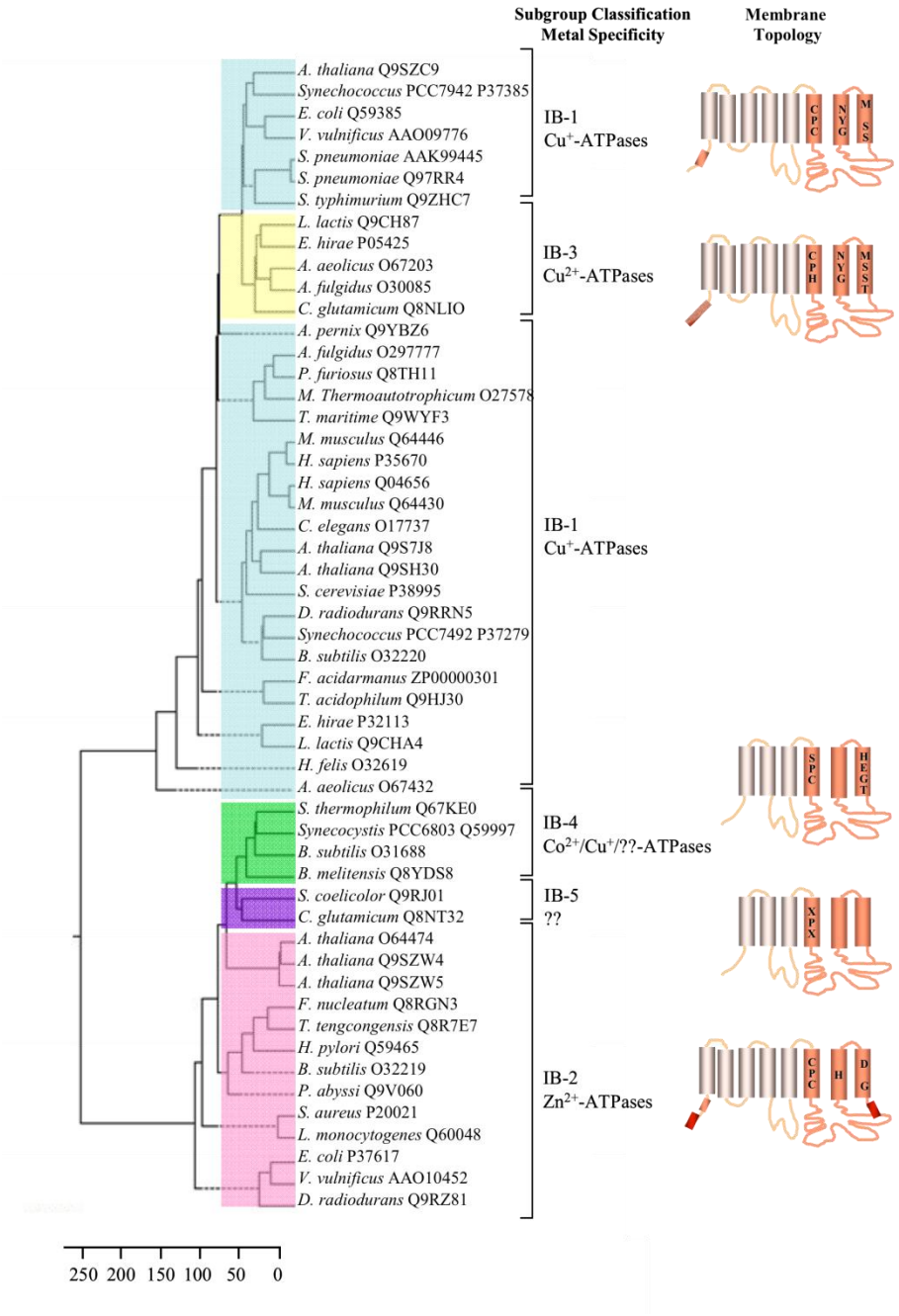

Fig. 5: Phylogenetic Tree of the P1B-type ATPases. The tree was prepared from a ClustalW alignment of representative sequences of P1B-type ATPases. The relative abundance of sequences from each subgroup has been maintained. The metal specificity and the structural characteristics are indicated next to the subgroup denomination. Amino acids in TMs are proposed to participate in determining metal selectivity. Black blocks represent His-rich N-MBDs; orange blocks, CXXC N-MBDs; and red, His and Cys rich N- and C-MBDs (This figure is published by Argüello et al., 2007[57]).

1.5 N AND C METAL BINDING DOMAINS

Besides TM-MBD most P_{1B}-ATPases have 1-6 cytoplasmic metal binding domains (MBD) located either in the N-terminus (N-MBD) or C-terminus or both (Tables 1 and 2). Most typical ones are the N-MBDs observed in Cu+-ATPases and bacterial Zn^{2+}-ATPases of subgroups IB-1 and IB-2. These are usually 60-70 amino acid domains characterized by a highly conserved CxxC sequence [29,46,58,59].

Table 1: Cytoplasmic N-terminus Metal Binding Domains of P_{1B}-ATPases (table has been presented in Eren. E thesis Dec 2006)

Type	Group[1]	Length[2]	Sequence	Protein
CXXC consensus	1B-1 1B-2	60-80	MVKDTYISSASKTPPMERTVRVTGMT **CAMC**VKSIETAVGSLEGVEEVRVNL ATETAFIRFDEKRIDFETIKRVIEDLGY GV	*A. fulgidus* CopA
CCXSE consensus	1B-2	90-100	MASKKMTKSYFDVLGI**CCTSE**VPLIE NILNSMDGVKEFSVIVPSRTVIVVHDT LILSQFQIVKALNQAQLEANVRVTGE TNFK	*A. thaliana* HMA2
$(HX)_n$ (n = 2-6)	1B-2	100-150	MNQPVS**HEHKHPHDHAHG**DDD**HGH** AA**HGHS**CCGAKAAPPLVQLSETASA QAQLSRFRIEAMDCPTEQTLIQDKLSK LAGIEQLEFNLINRVLGVRHTLDGTA DIERAIDSLGMKAEPIAAQDDGSASVP QPAKA	*P. putida* CadA-2
His rich	1B-3 1B-4	30-100	MNNGIDPENETNKKGAIGKNPEEKIT VEQTNTKNNLQE**H**GKMENMDQ**HH**T **H**G**H**MER**H**QQMD**H**G**H**MSGMD**H**S**H**M D**H**EDMSGMN**H**S**H**MG**H**ENMSGMD**H** SM**H**MGNFKQK	*E. hirae* CopB

1 Refers to subgroup classification showed in Figure 1.4.
2 Number of amino acids.

N-MBDs have been shown to receive metal from chaperones, however in Mtb there are no known chaperones that have been identified. Some zinc ATPases have histidine rich metal binding domains., similar sequences have been identified in ZIP (Zinc-regulated transporter, Iron-regulated transporter Protein) and CDF (Cation Diffusion Facilitator) families in the loops between transmembrane domains. Copper ATPases of subgroup P_{1B3} and a few members of P_{1B4} have a distinct His-rich metal binding domain instead of typical N-MBDs [29]. These domains have His stretches instead of Hx repeats.

Table 2: Cytoplasmic C-terminus Metal Binding Domains of P_{1B}-ATPases (table has been presented in Eren. E thesis Dec 2006)

Type	Group[1]	Length[2]	Sequence	Protein
Cys rich	1B-2	60-280	LNSMTLLREEWKGGAKEDGA**C**RAT ARSLVMRSQLAADSQAPNAADAGA AGREQTNG**C**R**CC**PKPGMSPEHSVVI DIRADGERQEERPAEAAVVAK**CC**GG GGGEGIR**C**GASKKPTATVVVAK**CC**G GGGGGEGTR**C**GASKNPATAAVVAK **CC**SGGGGEGIG**C**GASKKPTATAVVA K**CC**GGGGEGTR**C**AASKKPATAAVV AK**CC**GGDGGEGTG**C**GASKRSPPAEG S**C**SGGEGGTNGVGR**CC**TSVKRPT**CC** DMGAAEVSDSSPETAKD**C**RNGR**CC** AKTMNSGEVKG	*O. sativa* HMA3
Cys/His rich	1B-2	260-480	MLLLSDK**H**KTGNK**C**YRESSSSSVLIA EKLEGDAAGDMEAGLLPKISDK**HC**K PG**CC**GTKTQEKAMKPAKASSD**H**S**H**S G**CC**ETKQKDNVTVVKKS**CC**AEPVD LG**H**G**H**DSG**CC**GDKSQQP**H**Q**H**EVQV QQS**CH**NKPSGLDSG**CC**GGKSQQP**H** Q**H**ELQQS**CH**DKPSGLDIGTGPK**H**EG SSTLVNLEGDAKEELKVLVNGF**C**SSP ADLAITSLKVKSDS**HC**KSN**C**SSRER**C** **HH**GSN**CC**RSYAKES**C**S**H**D**HHH**TRA **H**GVGTLKEIVIE	*A. thaliana* HMA2

1 Refers to subgroup classification showed in Figure 1.4.
2 Number of amino acids.

Not all P_{1B} ATPases have a cytoplasmic MBD. This suggests that they are present for a regulatory function. Removal of N-MBD by truncation or inhibition of metal binding sites by mutation reduces enzyme activity with small changes in metal affinity. [60,61] [37,62-64] [65]. Previous experiments done in our laboratory has shown that N-MBDs of *Archaeglobulus fulgidus* Cu^{+}-ATPase CopA and Cu^{+2}-ATPase CopB control the enzyme turnover rate through the rate limiting conformational change associated with metal release/dephosphorylation[37,62]. Similar to the findings in copper ATPases it has also been found that Zinc ATPases (ZntA) also behave in a similar manner [66]. Truncation of either the N-MBD or C-MBD of *A. thaliana* Zn^{+2}-ATPase HMA2 results in a 50% decrease in enzyme activity with no significant change in metal affinity suggesting that both are regulatory domains [67]. Thus, we explored the N and C terminal sites of the Mtb ATPases to determine if they had any metal binding domains in these regions.

2. MATERIALS AND METHODS

2.1 IDENTIFICATION OF HOMOLOGS OF THE MTB ATPASES

A total of 192 sequences were analyzed to classify the Ctps in Mtb into the different categories based on the sequence similarity in helices H6, H7 and H8 in P_{1B} ATPases and H4, H5 and H6 in the P_2 ATPases. Online search tool NCBI's pBLAST[68] program was used.

2.2 IDENTIFICATION OF TRANSMEMBRANE HELICES

TM prediction tools were used from ExPASy (Expert Protein Analysis Systems) [69], they were SOSUI (Nagoya University, Japan) [70], TMPRED (EMBnet-CH) [71], HMMTOP (Hungarian Academy of Sciences) [72], DAS (Dense Alignment Surface method (Stockholm University)) [73] and PredictProtein™ (Columbia University) [74].

2.3 IDENTIFICATION METAL BINDING CONSERVED RESIDUES

Proteins identified by NCBI's pBLAST program were aligned using the software MegAlign™ from DNAStar™. Conserved residues were then identified in the TM regions using knowledge obtained from the previous analysis and mapping of these regions.

2.4 CLONING AND EXPRESSION OF CTP C AND CTP G

ctpC and ctpG cDNA were amplified by PCR from genomic DNA. Amplicons were ligated into pEXP5/NT-TOPO/His vector (Invitrogen, Carlsbad, CA). This vector introduced an N-terminal hexahistidine tag suitable for Ni^{2+} affinity purification. BL21Star™ *E. coli* cells (Invitrogen, Carlsbad, CA) were used for expressing ctpC and ctpG. Protein expression was induced with 1mM isopropyl D thiogalactoside (IPTG). A second construct of ctpC and ctpG was sub cloned into pBAD/TOPO/His vector (Invitrogen, Carlsbad, CA). This vector introduces a carboxyl terminal hexahistidine tag suitable for Ni^{2+} affinity purification and a V5 epitope for immuno-detection. The gene sequence was confirmed by automated DNA sequence analysis.

E. coli ΔCopA and ΔZntA (*E. coli* genetic stock centre at Yale University) have the CopA and ZntA genes mutated with a Kanamycin resistance cassette. These cells were transformed with the pEXP5/NT-TOPO construct for subsequent growth curve experiments.

For protein purification the BL21 cells were grown at 37ºC in 2 x YT media supplemented with 150 µg/ml ampicillin, 50 µg/ml chloramphenicol and expression induced with 1mM IPTG. Cells were harvested 3 h post-induction, washed with 25 mM Tris, pH 7.0, 100 mM KCl and stored at -70°C.

2.5 GROWTH CURVES

96 well plates were used to grow and analyze the growth of bacteria in different metal concentrations. The *E. coli* used were: BL21Star™, LMG194 ΔCopA and RW3110 ΔZntA. Empty vector was transformed into these strains to behave as controls. The cells were grown in

2x YT media to an OD_{600} of 0.6. Induced with 1mM IPTG for 1 hr. The cells were harvested by centrifugation at 5,000g for 5 minutes and resuspended in media containing 2x YT, 100 µg/ml Ampicillin and 0.1mM IPTG, for LMG194 ΔCopA and RW3110 ΔZntA, 50 µg/ml Kanamycin was used besides ampicillin to maintain the mutation. The cells are diluted to an OD_{600} of 0.2 in the same media and transferred to the 96 well plates containing 10µl of the required metal. OD_{600} was obtained at indicated intervals and the results were analyzed using Microsoft Excel™ and Kaliedagraph™ from SynergySoftware™.

2.6 HEAVY METAL INIBITION ASSAY

2x YT Agar plates (2% Agar) were prepared, a layer of Top Agar (< 0.7% Agar) of 3 ml volume was maintained at a temperature of 55 ºC in a water bath. BL21Star™ cells with ctpC in pEXP5/NT-TOPO were induced with 1mM IPTG for 1 hr, harvested and resuspended in media containing 2x YT, 100 µg/ml ampicillin and 0.1mM IPTG. The cells were diluted to an OD_{600} of 0.2 in Top Agar kept at 55 ºC. The cooled agar plates were then distributed with 3 ml of the Top Agar + ctpC BL21Star™ cells and Top Agar + pEXP5/NT-TOPO BL21Star™ cells.

Whattman No.1 Filter Paper Discs (0.5 cm) were loaded with the desired quantity of metal and placed on the top Agar with sterile double-autoclaved and flamed forceps. Water or water with ascorbic acid was used as a control. The plates were placed at room temperature to cool down and then placed at 37 ºC overnight. Inhibition halos were observed in the lawn of bacteria that grew overnight on the plates. These were photographed and measured. The empty vector cells were compared with the cells with the insert.

2.7 METAL CONTENT IN *E. COLI* EXPRESSING CTP C AND CTP G

E. coli cells expressing CtpC and CtpG, and cells transformed with empty vector, were grown in 2x YT media overnight. The cells were then transferred to fresh media and grown to an OD_{600} of 0.6. The cells were induced for 3 hrs with 0.002% Arabinose. Cells were harvested by centrifugation, and washed 3 times with water. Cells were disrupted by sonication, protein content was analyzed using Bradford method [75]and subjected to ICP-MS analysis [76].

2.8 CTP C PROTEIN EXPRESSION AND PURIFICATION

Protein purification was carried out as previously described [77]. All purification procedures were carried out at 0-4 ºC and no special precautions were taken to prevent enzyme oxidation. Cells were suspended in buffer A (25 mM Tris, pH 7.0, 100 mM sucrose, 1 mM phenyl methyl sulfonyl fluoride (PMSF)) and disrupted by passing them through a French Press 3 times at 20,000 p.s.i.. Lysed cells were centrifuged at 8,000 x g for 30 min. The supernatant was then centrifuged at 163,000 x g for 1 h, the pellet washed with buffer A, and centrifuged at 229,000 x g for 1 h. Membranes were resuspended in buffer A (10-15 mg/ml) and stored at -70°C. For protein solubilization and purification, membranes (3 mg/ml in buffer B: 25 mM Tris, pH 8.0, 100 mM sucrose, 500 mM NaCl, 1 mM PMSF) were treated with dodecyl-β-D-maltoside (DDM) (Calbiochem, San Diego, CA), added drop wise to a final concentration of 0.75%. The membrane preparation was incubated with the detergent for 1 h at 4°C with mild agitation. The suspension was cleared by centrifugation at 229,000 x g for 1 h and Ni^{2+}-nitrilotriacetic acid (Ni-NTA) resin (Qiagen, Valencia, CA) pre-equilibrated with buffer B plus 0.05% DDM, 5 mM imidazole was added to the supernatant. After incubation for 1 h at 4°C, the resin was placed on a column and washed with buffer B, 0.05% DDM, 20 mM imidazole. The protein was eluted

with buffer B, 0.05% DDM and 200 mm imidazole. Fractions were concentrated by filtration in 50,000 MW centricon (Millipore, Billerica, MA) and imidazole was removed using a Sephadex G-25 column. The protein was eluted with 25 mM Tris, pH 8.0, 100 mM sucrose, 50 mM NaCl, 0.01% DDM, 10% glycerol and stored in this buffer at -70°C. All protein determinations were performed in accordance with Bradford[75].Protein expression and purification was examined on 10% SDS-PAGE [78]. Expression of the proteins was observed by staining the gels with Coomassie Brilliant Blue and immunobloting using Anti-His6 Epitope Tag Antibody (Rabbit Polyclonal IgG) and Goat Anti-Rabbit IgG Antibody (horseradish peroxidase conjugate) (GeneScript Corporation, Piscataway, NJ).

2.9 pNPPase ASSAY OF CTP C

pNPPase activity assays were carried out as previously described[79]. pNPPase activity assay mixture contained 50 mM Tris, pH (75 ºC) 6.1, 3 mM MgCl2, 3 mM ATP, 0, 2, 10, 20 or 50 mM Cys, 0.01% asolectin, 0.01% DDM, 400 mM NaCl, 0.01 mg/ml purified enzyme, and different concentrations of metal was used. The buffer was prepared at room temperature and pH 7. pNPPase activity was measured for 10 min at 37 °C.

3. RESULTS

3.1 P-TYPE ATPASES IN MTB

The focus of our study has been to understand the structure and function of Mtb ATPases. In particular we wanted to study the P-type ATPases that are known to transport heavy metals. We wanted to deduce a possible function for these ATPases regarding conserved residues found on the TM helices after sequence alignment with other known ATPases. We have conducted a bioinformatics analysis of the twelve P-ATPases of Mtb. Interestingly, most of these proteins cannot be associated with the subgroups described earlier (Fig. 4). This is surprising since most microorganisms contain a P_{1A}-type K^+-ATPases and one or two P_{1B}-ATPase genes, usually Cu^+ or Zn^{2+}-ATPases (P_{1B1} and P_{1B2} subgroups). Based on the previously observed conserved residues, we could identify that ctpA, B and V are Copper ATPases of subgroup P_{1B1}. They are present in all the known mycobacterial genomes (*M. avium, M. bovis, M. bovis BCG, M. leprae, M. marinum, M. semegmatis, M. ulcerans*).

Ctps A, B and V belong with the same group as the Cu^+/Ag^+-ATPases. Proteins that belong with this subgroup are found in eukaryotes, prokaryotes and archea. These include Menkes' and Wilson disease proteins, which are, associated with genetic Cu transport disorders in humans [26,80] [81,82]. For example, *Arabidopsis thaliana* RAN1 [83] [84], *E. coli* CopA [36] [77] [30] and *A. fulgidus* CopA have been shown to transport non-physiological substrate Ag^+ and drive the efflux of the metal from the cytoplasm [85] [77]. Proteins of this subgroup have a conserved CPC in TM H6, in addition, these proteins contain conserved residues, Asn, Tyr in TM H7 and Met, Ser in TM H8.

CtpC aligned closer to CtpV than to CtpA or B (Fig. 6). It looks like a mutated copper ATPase as it has a Met in TM H8 replaced with a His. CtpG has APC instead of CPC in TM H6, which leads to other possible substrates for this protein. CtpJ and D have a SPC in TM H4, which classifies them to the P1B4 subgroup. Members of this group have only 6 putative TMs [23]. Of these, the large cytoplasmic loop containing the DKTGT sequence is located between TM H4 and H5. The substrate specificity of these enzymes has not been characterized. Further characterization studies of other members are necessary to state the metal specificity of subgroup 1B-4 proteins.

Previously no proteins from Mycobacteria were found in P_{1B5} subgroup. However there are some proteins from this genus (other than Mtb) that were found to belong to this subgroup. Ctps E, F, H and I belong to the P_2 ATPases. They have to yet be classified into subgroups.

As a starting point toward formulating relevant hypothesis on the functional role of these ATPases, we analyzed their topology, presence of signature amino acids, and putative substrate specificity (Table 3). Additionally, homologs of the Mtb P-ATPases were identified, using protein BLAST searches, (last column in Table 3). Except the Cu^+ ATPases (CtpA, CtpB and CtpV) and the K^+-ATPases KdpB, the other sequences are found in symbiotic bacteria (pathogenic or beneficial) and some chemolithotrophic archaea and bacteria.

KdpB: Is a multi subunit protein present only in prokaryotes, it drives K^+-efflux. The *E. coli* homologue has been well characterized [86].

CtpV, CtpB, and CtpA: Are typical Cu^+-ATPases. They contain Cu^+ coordinating signature sequences in their TMs. They are highly homologous (40-56% identity). Mutation of homologous genes in *Pseudomonas aeruginosa* and Listeria *monocytogene*s reduces their virulence [87] [88].

Table 3: P-type ATPases in Mtb

Name	Gene	Swiss Prot	Length	Selectivity	TM	Subfamily	Other Mycobacteria	No. of Seq	Other Organisms
CtpG	Rv1992c	P63689	771	Heavy metal?	8	P1B?	B,C,M	3	Legionella pneumophila, M.bovis
CtpJ	Rv3743c	O69710	660	Co/Mn/Cu?	6	P1B4	B,C,M,S,U	30	Listeria monocytogenes
CtpD	Rv1469	P63685	657						Mycobacterium gilvum
CtpC	*Rv3270*	P0A502	718	Cu^+/heavy metal?	8	P1B?	A,B,C,L,M,S,U	8	Bacillus subtilis, B.anthracis
CtpV	*Rv0969*	P77894	770						Clostridium botulinum
CtpB	*Rv0103c*	Q10877	752	Cu^+	8	P1B1	A,B,C,L,M,S,U	>100	Staphylococcus aureus
CtpA	*Rv0092*	Q10876	761						Staphylococcus epidermidis
CtpE	*Rv0908*	P0A504	797	Alkali metal?	10	PII?	A,B,C,M,U,S	40	Clostridium botulinum
CtpF	*Rv1997*	P63687	905					52	
CtpH	*Rv0425c*	A5TZF1	1539	Alkali metal?	10	PII?	A,B,C,L,M,S,U	30	Clostridium thermocellum
CtpI	*Rv0107c*	Q10900	1625					29	Lactobacilus acidophillus
kdpB	*Rv1030*	P63681	709	K^+	8	P1A	A,B,C,L,M,S,U	>100	Bradyrhizobium japonicum

A-Mycobacterium avium/paratuberculosis
B-Mycobacterium bovis
C-Mycobacterium bovis BCG
L-Mycobacterium leprae
M-Mycobacterium marium
S-Mycobacterium smegmatis
U-Mycobacterium ulcerans

CtpC: Is homologous (26-36% identity) to Cu^+-ATPases (CtpV, B, and A). However, two key Cu^+ binding residues are not conserved. It may thus be involved in transporting another metal. Alternately, transport of Cu^+ with a 1 Cu/ATP (rather than 2 Cu/ATP) **[89]** can be hypothesized.

CtpJ and CtpD: These are members of the P_{1B4} subgroup. Studies of *Synechocystis* CoaT suggest that these are Co-ATPases [90]. Studies of Arabidopsis HMA1, containing identical metal coordinating residues, have proposed that this is a Cu^+-ATPase [91] or a Ca-ATPase [92]. Functional complementation studies of AtHMA1, carried out by previous members in our lab, suggest that members of this group belong to the Mn-ATPases. Clearly, these are heavy metal transporting ATPases, their specificity is still to be determined.

CtpG: This is a rare ATPase. We could identify only two homologous sequences, in *M. bovis* and *Legionella pneumophila*. It has the topology of P_{1B}-ATPases with the typical DKTGT sequence in the ATPBD, but no other characteristic allows its association with any particular subgroup.

CtpE and CtpF: Their membrane topology corresponds with that of P_2 or P_3-ATPases (Fig. 1) but they do not appear to have residues conserved in ATPases of known substrate, except for a conserved Glu in H4. This Glu is characteristic of P_2 and P_3 ATPases and it is absent in P_{1B}-ATPase [24 45 93 94]. We hypothesize that these might transport an alkali metal, protons, or perhaps ammonium.

CtpH and CtpI: These are similar to CtpE and CtpF; however, they have a long (>600 aa) N-terminal fragment present only in homologous bacterial P-ATPases.

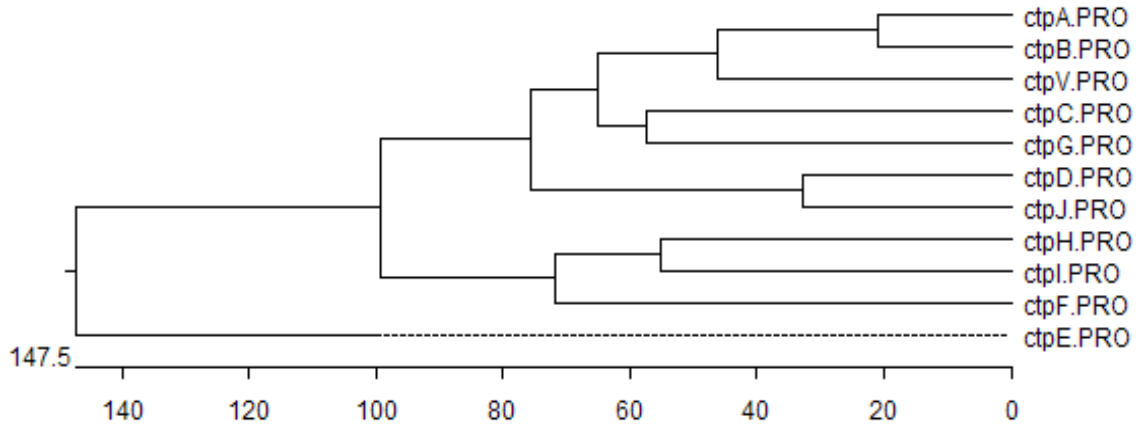

Fig. 6: Dendrogram depicting the homology of the Ctps.

As a part of this work, we have studied the N and C terminal domains for the Mtb ctps. No conserved residues were observed in the N-terminal or C-terminal domains of the Mtb ctps. This could mean that there is no conservation of function of these domains from the known P-type ATPases. This is strange because Mtb like *E. coli* does not possess any known chaperones for transporting heavy metals. The N and C terminal domains of CopA for example have a regulatory role in the enzyme's function. The regulation of these Mtb Ctps is not known and has to be determined by further studies.

3.2 GENOMIC ORGANIZATION OF MTB CTPS

The roles and functionality of these genes can be hypothesized by looking at their operons. This gives us an idea of what genes are co-expressed with the gene of interest. ctpC in Fig. 7 shows these putative functional units for genes of interest. CtpC is co-expressed with flanking genes related to cell synthesis. Alternately, CtpG and CtpV appear co-expressed with stress response transcriptional regulators that belong with the ArsR and CsoR families respectively. It is possible that these genes are co-expressed when Mtb ctps are expressed in response to stress that is encountered in the phagosolysosome. Microarray analysis that was conducted on the 194 genes present in Mtb [95] [96]has identified ctpC, G and F to be elevated when there is stress experienced by the bacteria in the macrophage.

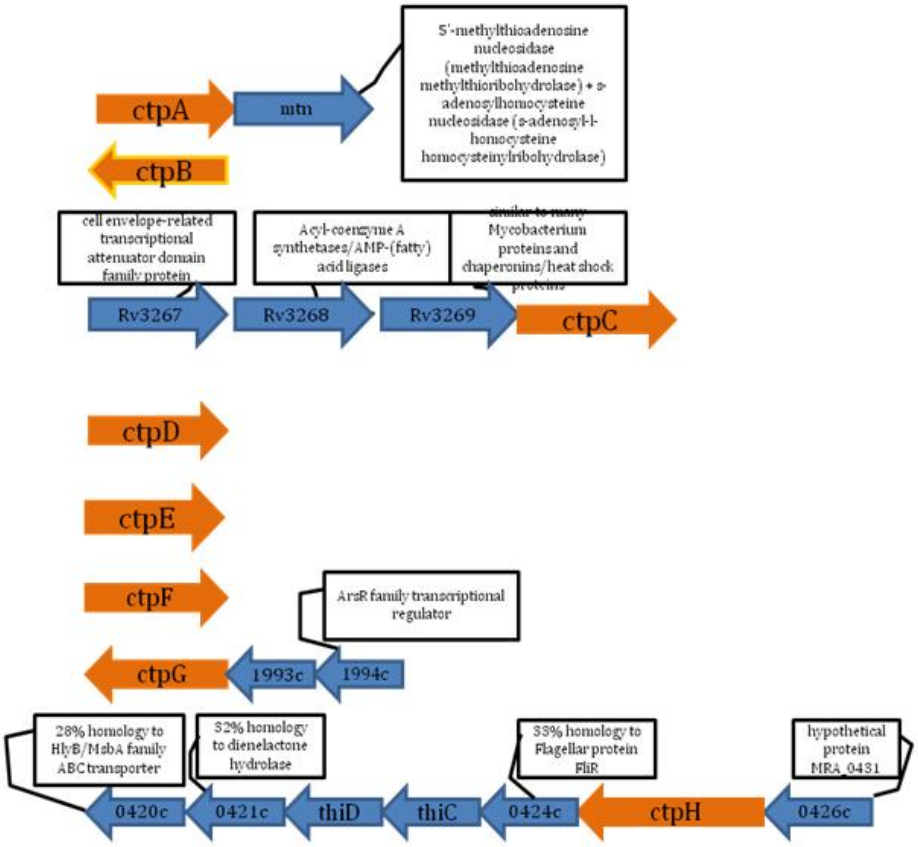

Fig. 7: Figure showing the genomic organization of the ctps.

3.3 HOMOLOGS OF CTPS IDENTIFIED IN OTHER ORGANISMS

A through bioinformatic analysis was performed on the 12 P-type ATPases of Mtb. We have attempted to characterize these proteins in to subgroups based on the conserved sequences found in the different domains. Using a pBLAST search homologs were identified in other organisms. It was noticed that there was an abundance of these proteins in symbiotic, pathogenic and chemolithotrophic archea and bacteria. (Table 4)

Type	Swiss Prot	Other organisms
CtpG	P63689	Legionella pneumophila
		Mycobacterium bovis
		Sulfurovum sp. NBC

Type	Swiss Prot	Other organisms	Other organisms	Other organisms	Other organisms
CtpJ	O69710	Lyngbya sp.	Novosphingobium aromaticivoran:	Erythrobacter litoralis	Caulobacter sp. K31
CtpD	P63685	Anabaena variabilis	Bacillus cereus	Exiguobacterium sibiricum	Chlamydophila abortus
		Arabidopsis thaliana	Bacillus halodurans	Gramella forsetii	Chlamydophila caviae
		Bacillus licheniformis	Bacillus subtilis	Hyphomonas neptunium	Chlamydophila felis
		Caulobacter crescentus	Bacillus weihenstephanensis	Acidovorax sp. JS42	Flavobacterium sp. MED217
		Corynebacterium efficiens	Chlamydia muridarum	Aster yellows witches'-broom phytoplasma	Listeria welshimeri
		Erythrobacter sp. NAP1	Chlamydia trachomatis	Bradyrhizobium sp. BTAi1	Mycobacterium bovis
		Lactobacillus casei	Chlamydophila pneumoniae	Burkholderia multivorans	Mycobacterium ulcerans
		Mycobacterium sp. KMS	Enterococcus faecalis	Acidovorax sp. JS42	Nocardia farcinica

Type	Swiss Prot	Other organisms	Other organisms
CtpC	P0A502	Kineococcus radiotolerans	Clostridium Bartletti
		Methanosarcina acetivorans	Mycobacterium marinum
		Methanosarcina barkeri	Mycobacterium smegmatis
			Mycobacterium ulcerans

Type	Swiss Prot	Other organisms	Other organisms
CtpV	P77894	Bacillus anthracis	Desulfotomaculum reducens
CtpB	Q10877	Bacillus cereus	Geobacillus kaustophilus
CtpA	Q10876	Bacillus coagulans	Heliobacillus mobilis
		Bacillus subtilis	Oceanobacillus iheyensis
		Clostridium botulinum	Thermoanaerobacter ethanolicus
		Clostridium perfringens	Thermoanaerobacter tengcongensis
		Clostridium tetani	Bacillus thuringiensis
		Clostridium thermocellum	Mycobacterium bovis
		Enterococcus faecalis	Mycobacterium ulcerans
		Moorella thermoacetica	Bacillus licheniformis
		Staphylococcus aureus	Symbiobacterium thermophilum
		Staphylococcus epidermidis	Syntrophomonas wolfei
		Caldicellulosiruptor saccharolyticus	Bacillus amyloliquefaciens

Type	Swiss Prot	Other organisms	Other organisms
CtpE	P0A504	Clostridium botulinum	Arthrobacter sp
		Clostridium thermocellum	Clostridium beijerinckii
		Lactobacillus plantarum	Mycobacterium bovis
		Mycobacterium smegmatis	Mycobacterium ulcerans
		Streptococcus pneumoniae	Mycobacterium avium
		Streptococcus sanguinis	Rhodococcus sp. RHA1
		Streptococcus thermophilus	Acidothermus cellulolyticus
		Mycobacterium sp. JLS	Synechococcus sp. JA-3-3Ab
		Mycobacterium sp. MCS	Trichodesmium erythraeum
		Mycobacterium gilvum	Marinobacter aquaeolei
		Mycobacterium vanbaleenii	

Type	Swiss Prot	Other organisms	Other organisms	Other organisms	Other organisms
CtpF	P63687	Desulfotomaculum reducens	uncultured archaeon GZfos12E1	Pelobacter propionicus	Yersinia enterocolitica
		Desulfovibrio vulgaris	Methanococcoides burtonii	Pseudoalteromonas atlantica	Yersinia pseudotuberculosis
		Geobacter lovleyi	Mycobacterium bovis	Rhodopseudomonas palustris	Acidovorax sp. JS42
		Halorhodospira halophila	Mycobacterium ulcerans	Salinispora arenicola	Alkalilimnicola ehrlichei
		Mycobacterium sp. JLS	Nitrosomonas europaea	Syntrophobacter fumaroxidans	Azoarcus sp.
		Mycobacterium sp. MCS	Yersinia pestis	Psychromonas ingrahamii	Nitrosomonas eutropha
		Mycobacterium vanbaleenii	Pseudomonas aeruginosa	Dinoroseobacter shibae	Marinobacter aquaeolei
		Nostoc sp.	Pseudomonas mendocina	Synechococcus sp.	Parvibaculum lavamentivorans
		Paracoccus denitrificans	Pseudomonas stutzeri	Thermoanaerobacter ethanolicus	

Type	Swiss Prot	Other organisms	Other organisms
CtpH	15607566	Clostridium cellulolyticum	Mycoplasma penetrans
Ctpi	Q10900	Lactobacillus sakei	Pseudomonas stutzeri
		Chlorobium phaeobacteroides	Streptococcus agalactiae
		Geobacter bemidjiensis	Synechococcus sp.
		Geobacter uraniumreducens	Thermofilum pendens
		Halorhodospira halophila	Caldicellulosiruptor saccharolyticus
		Mycobacterium sp. JLS	Acidiphilium cryptum
		Mycobacterium vanbaleenii	Chloroflexus aggregans
		Nostoc sp.	methanogenic archaeon RC-I
		Roseiflexus castenholzii	Methanothermobacter thermautotrophicus
		Roseiflexus sp	Psychromonas ingrahamii
		Salinispora arenicola	Halothermothrix orenii
		Salinispora tropica	Shewanella frigidimarina
		Schizosaccharomyces pombe	Mycobacterium avium
		Burkholderia xenovorans	Mycobacterium bovis
		Lactobacillus acidophilus	Mycobacterium ulcerans
		Lactobacillus plantarum	Rhodococcus sp. RHA1
		Clostridium thermocellum	Marinobacter aquaeolei
		Mycobacterium leprae	Parvibaculum lavamentivorans

KEY:	Animal Pathogen	involved in Bioremidiation/Biotechnology
	Plant Pathogen	
	Grow in Hot springs/with chemical energy	
	Human Pathogen	

Table 4: Homologous sequences found in other organisms.

3.4 MTB HAS MORE P-TYPE ATPASES THAN MOST KNOWN ORGAMISMS

A sample set of organisms was considered to analyze the number of P-type ATPases they possess. It was observed that most of the organisms had 1-2 ATPases or sometimes even 3. *M. bovis* showed 4 ATPases that were present in Mtb. (Table 5)

	P1B4	P1B6	CtpC	CtpE	CtpF	CtpH/I	CtpV/B/A	
Acidiphilium cryptum						1		1
Bacillus anthracis							1	1
Bacillus coagulans			1				1	2
Bacillus subtilis	1		1				1	3
Bacillus thuringiensis	1		1				1	3
Bradyrhizobium sp. BTAi1	1							1
Brucella melitensis	1							1
Clostridium botulinum			1	1			1	3
Clostridium difficile			1					1
Clostridium tetani							1	1
Heliobacillus mobilis			1				1	2
Mycobacterium bovis				1	1	1	1	4
Mycobacterium gilvum	1			1				2
Pseudomonas aeruginosa					1			1
Ralstonia metallidurans	1							1
Staphylococcus aureus	1						1	2
Staphylococcus epidermidis							1	1
Streptococcus pneumoniae				1				1
Synechococcus sp.					1	1		2
Thermoanaerobacter sp.			1		1		1	3
Thermofilum pendens						1		1
Yersinia pestis					1			1

Table 5: Maximum number of P-type ATPases in other organisms.

3.5 METAL BINDING CONSERVED RESIDUES IN TRANSMEMBRANE HELICES WERE IDENTIFIED

Once the different metal binding helices were identified, they were aligned with their homologs from other organisms and consensus sequences in each set was identified along with other TM helices. (Table 6)

	Mtb Ctp	#TM	Consensus Seq				
			H4	H5	H6	H7	H8
P1B6	CtpG	8			APC	QN	HEx(T/S)E
P1B4	CtpJ	6	SPC	'N	HEGST		
	CtpD	6	SPC	N	HEGST		
P1B5		7		TPCP	S xxx M	QE X D	
P1B	CtpC	8			CPC	NY	HxxSS
P1B1	CtpV	8			CPC	NY	MxxSS
P1B1	CtpB				CPC	NY	MxxSS
P1B1	CtpA				CPC	NY	MxxSS
P2	CtpE	10	PEGL	GR N LxK	PxxP (S/T) GxPxFxL		
P2	CtpF	10	PEGLP	NxxK	P QxLWxN		
P2	CtpH	10	PEGxP	NxGE	LxxN A		
P2	Ctpi	10	PEGLP	NxGE	LxxN		

Table 6: Conserved residues identified in each helix.

Interestingly there were no Mtb proteins identified as P1B5, but there were other Mycobacteria like *M. gilvum, M. sp. MCS* and *M. vanbaalenii* that were identified with P_{1B5} proteins. Ctps E, F, H and I resembled potassium, sodium or calcium ATPases. They were hence compared with calcium ATPases from P_{2A} and P_{2B}, Proton Potassium ATPases from P_{2C}, Sodium Potassium ATPases from P_{2C}, α subunits of P_{3A} and P_{3B} ATPases.

It was observed that ctpE had around 20% homology to Manganese calcium ATPases and P3A ATPases. CtpF is 33% homologous to Manganese calcium ATPases. ctpH is 27% homologous to P_{3A} ATPases and ctpI is 20% homologous to Manganese Calcium ATPases and 19% homologous to P_{3B} ATPases. It can be deduced that ctpE and F can be similar to ctpH and I except for the stoichiometry. (Fig. 8)

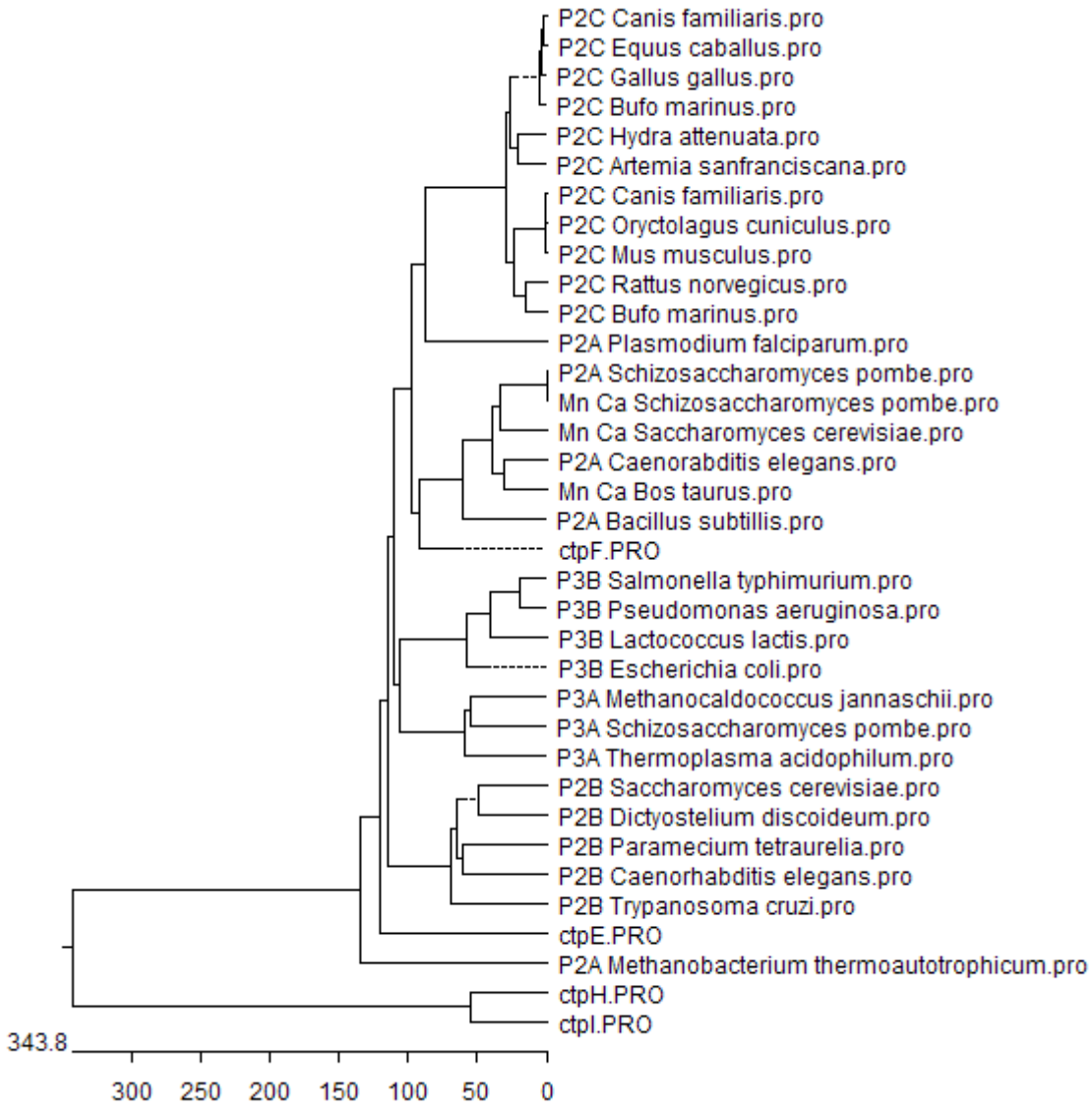

Fig 8: Homology of ctpE, F, H and I to other P_2 and P_3 ATPases.

Additionally the N and C terminal domains were analyzed for conserved metal binding domains ctpA and B did not have a significant C terminal cytoplasmic domain. This is consistent with the copper ATPases that are seen in *E. coli* like CopA. There was a glycine, arginine rich region observed in ctpE. But nothing significant was observed in the C terminal cytoplasmic domains of the Mtb Ctps. (Table 7)

	Mtb Ctp	#TM	N-terminal Domain	C Terminal Domain
P1B6	CtpG	8	W	R G
P1B4	CtpJ	6	**NCI**	**NCI**
	CtpD	6	**NCI**	**NCI**
P1B5		7	**NCI**	**NCI**
P1B	CtpC	8	R S	SxRLIxY
P1B1	CtpV	8	**NCI**	**NCI**
P1B1	CtpB		CxxC	**NCI**
P1B1	CtpA		CxxC	**NCI**
P2	CtpE	10	GL G N I N T N L GL V R G N	**NCI**
P2	CtpF	10	G R GxN	**NCI**
P2	CtpH	10	**NCI**	**NCI**
P2	Ctpi	10	**NCI**	**NCI**

NCI=No consensus identified

Table 7: Conserved residues in the N and C terminal domains.

3.6 ANALYSIS OF THE ROLE OF CTP C

The strains BL21Star™, LMG194 ΔCopA and RW3110 ΔZntA were used for obtaining the growth curves. The cells were grown in 96 well plates. The cells grown in No metal and no metal + ascorbate showed no difference when compared with cells transformed with empty vector. This showed that the cells were behaving normally. Differences were observed in 750 µM copper (Fig. 9A), 125 µM cadmium (Fig. 9B), 750 µM Iron (Fig. 9C).

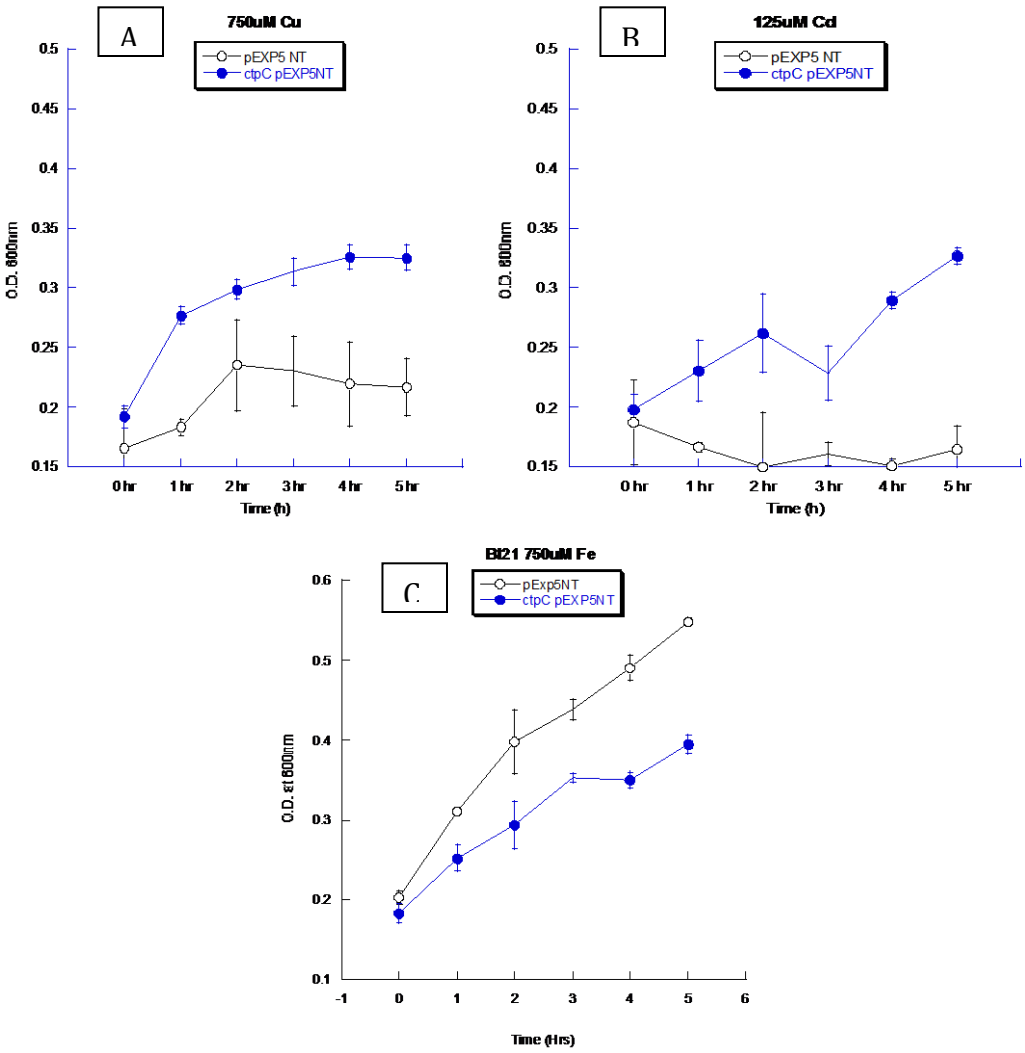

Fig 9: Differences observed in growth curves with Cu, Cd and Fe in BL21 cells. (*n=3)

The cells expressing ctpC appear to be more resistant to Cu^{2+} and Cd^{2+}. In Iron, however the cells expressing ctpC seemed to be more sensitive than the cells with the empty vector. The cells were also grown in different pHs of 5.5, 6, 6.5 and 7. No differences were observed in their growth curves.

LMG194 ΔCopA and RW3110 ΔZntA with the empty vector and ctpC were then subjected to the same metal concentrations to observe a difference. ctpC showed a difference with RW3110 ΔZntA strain, at 125 µM Cd (Fig. 10A) and LMG194 ΔCopA strain at 750 µM Cu (Fig. 10B).

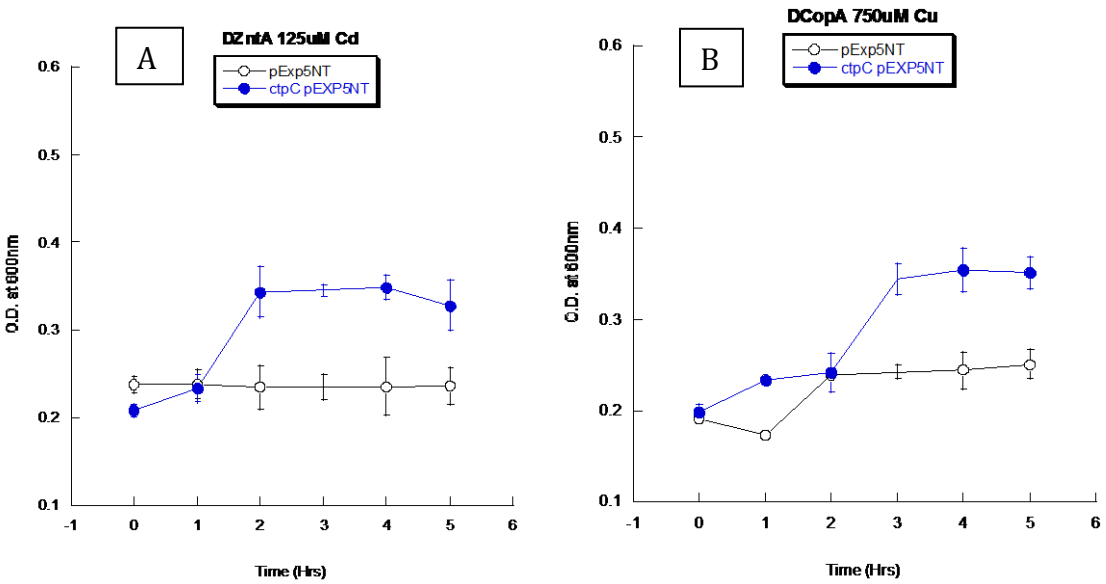

Fig 10: Differences observed in growth curves with Cu and Cd with LMG194 ΔCopA and RW3110 ΔZntA cells. (*n=3)

Further studies need to be done to elucidate the true substrate for ctpC.

3.7 HEAVY METAL INHIBITION ASSAY SHOWED A DECREASE IN INHIBITION ZONE FOR CADMIUM, NICKEL AND COPPER

Heavy metal inhibition assays were perform on 2x YT agar plates as described in the material and methods. There was a significant reduction in the inhibition zones observed for Cadmium (Fig. 11A), Nickel (Fig. 11B) and Copper (Fig. 11C).

Cadmium 1M

A

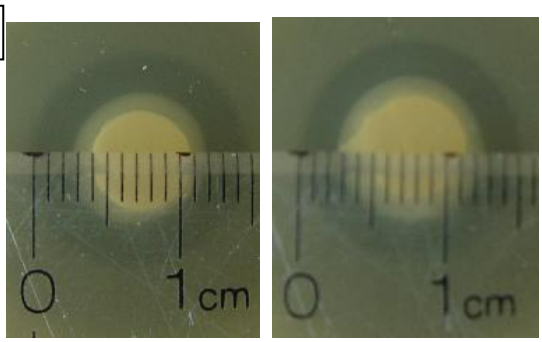

pEXP5/NT ctpC+ pEXP5/NT

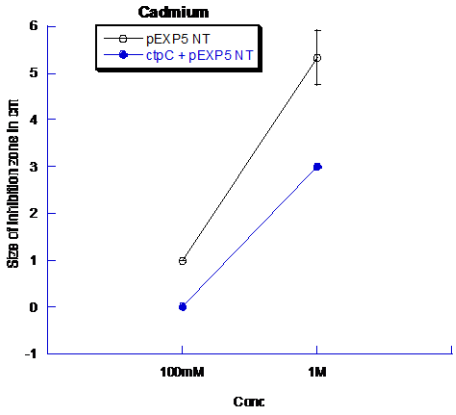

Nickel 1M

B

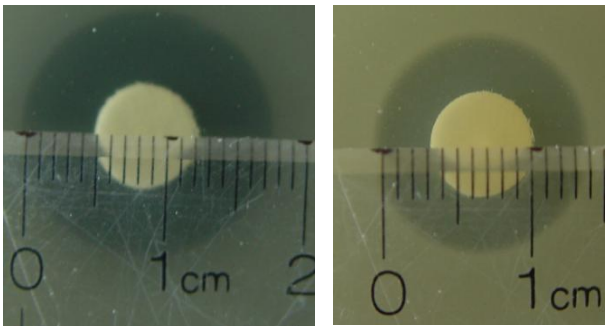

pEXP5/NT ctpC+ pEXP5/NT

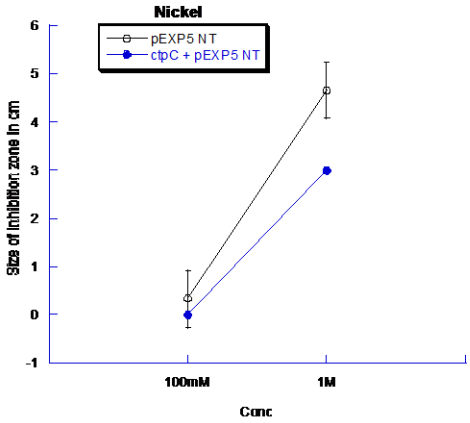

Copper 1M

C

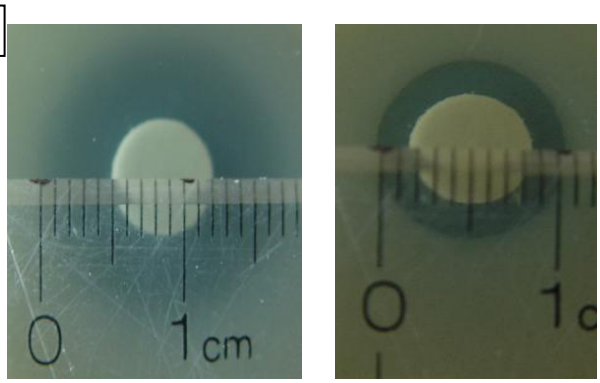

pEXP5/NT ctpC+ pEXP5/NT

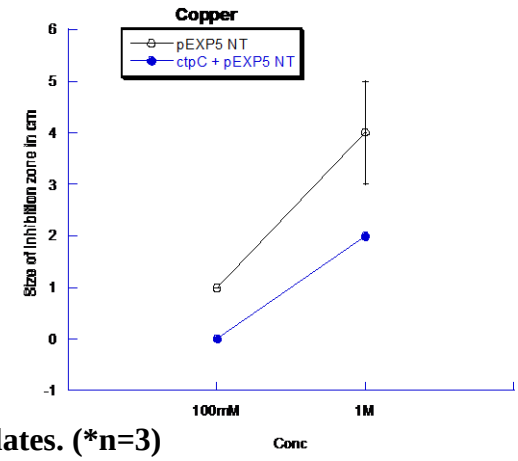

Fig 11: Heavy metal inhibition assay on 2x YT agar plates. (*n=3)

3.8 CTP C AND CTP G EXPRESSING E. COLI SHOW ACCUMULATION OF COBALT IN CTP G

The Top10 cells that were grown and induced for protein production were then subjected to nitric acid digestion, the results were analyzed by ICPMS analysis.

It was observed that cells expressing ctpC retained Molybdenum and Manganese (Fig. 12), while ctpG significantly retained Cobalt (Fig. 12). The data obtained pertaining to ctpC was inconsistent with what was observed in previous liquid and agar experiments.

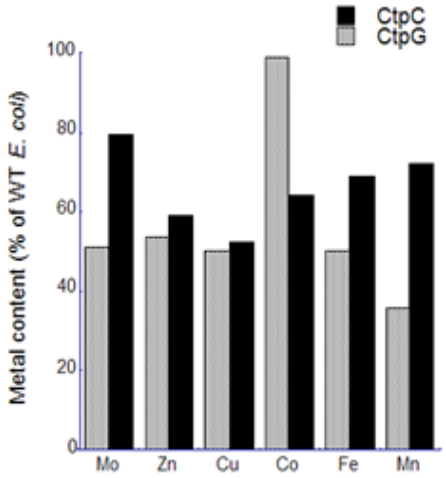

Fig 12: Heavy metal quotas of *E. coli* transformed with ctpC and ctpG. Data normalized by protein content and expressed as a percent of the content in *E. coli* transformed with empty vector (*n=1).

3.9 CTP C WAS CLONED AND EXPRESSED FOR PRODUCTION OF PURE PROTEIN

ctpC and ctpG were amplified from genomic Mtb H37Rv DNA (Fig. 13) , cloned into pCRT7/NT-TOPO/His vector and transformed in BL21 cells. Fig. 14 shows the purified protein isolated from the corresponding cells after induction with IPTG. To purify the protein, the membrane fraction was solubilized with 0.75% DDM under conditions in which maximal enzymatic activities were retained.

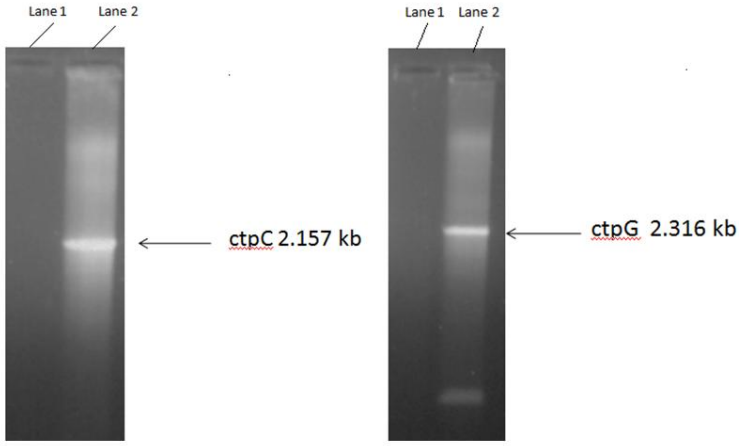

Fig. 13: PCR Amplification of CtpC and CtpG: Lane 1 indicates negative control and Lane 2 indicates the amplified DNA.

The solubilized proteins were subsequently purified by Ni^{2+}-NTA affinity column. These purification procedures yielded pure ctpC as judged by Coomassie Brilliant Blue-stained SDS PAGE gel (Fig. 14). The immunostained western blot showed that the protein was obtained in the pure form .

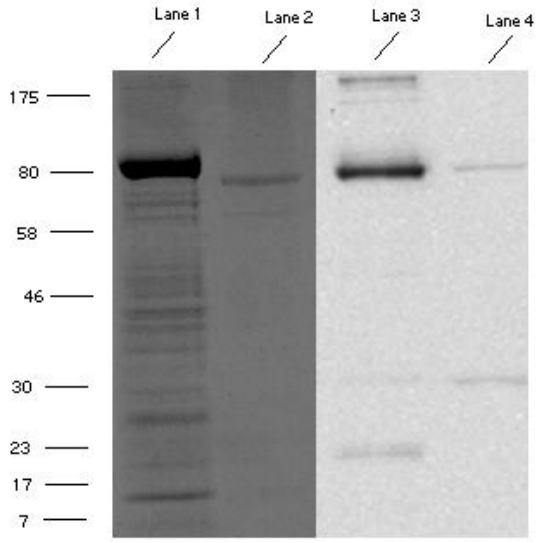

Fig. 14: Expression of Pure protein for ctpC. Lane 1 is 10µg of protein loaded onto an SDS-PAGE gel. Lane 2 is a His tag protein (ΔC CopA) used as a positive control for the Western blot. Lanes 3 and 4 are the western blot of the Protein gel.

3.10 pNPPase ASSAY SHOWED INHIBITION BY MANGANESE AND COBALT

pNPP assay was performed at 37 °C for different metals at 1, 10 and 100 µM metal concentrations. The absorbance read at 410nm was then plotted against the metal concentration (Fig. 15). It was observed that cobalt and manganese inhibited the enzyme. Metals that inhibit enzyme activity in the pNPP assay are known to activate the ATPase assay. Thus, this may mean that cobalt or manganese could be the possible substrates. This assay has been performed only once and has to be repeated to produce more conclusive results. Subsequently an ATPase assay will provide proof of the activity by a particular metal. The results seen in this assay however does not complement the results from the studies performed in *E.coli*. Activation by copper and zinc however prove that the enzyme has phosphatase activity, but no conclusive results can be drawn.

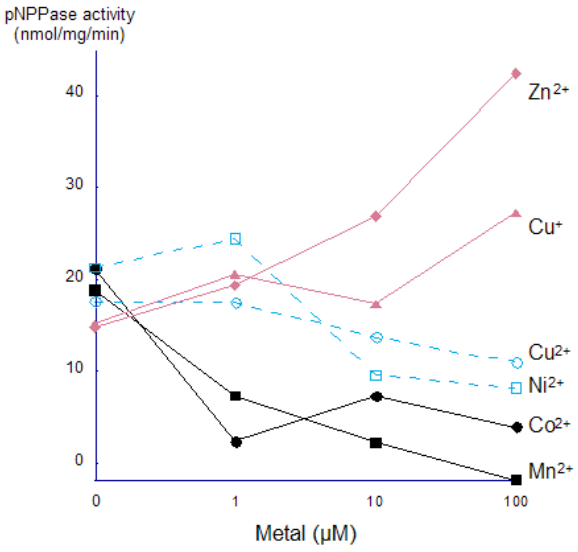

Fig. 15: pNPP activity of ctpC with different metals. pNPPase for ctpC activity is indicated in nmol/mg/min. (*n=1)

4. SUMMARY

Macrophages are central to host defense against microbes. Intracellular pathogens like Mtb have evolved to evade the body's antimicrobial functions. Mtb has successfully exploited macrophages as its primary niche *in vivo*, but the requirements for its intracellular survival remain undefined [97]. Virulent Mtb can replicate within the hostile environment of macrophages, and survive in poorly acidified phagosomes that fail to fuse with lysosomes [98].

The genome of Mtb shows the presence of 12 metal transporting P-type ATPases. Homologs of these ATPases have been identified in other pathogenic and symbiotic organisms. This proves that metals are required for interactions within the complex host-pathogen environments. Mtb genome also encodes SODs and other metal requiring enzymes, which are pumped into the noxious environment of the phagolysosome to protect the bacillus. Copper, zinc and manganese are known to be the metal co-factors in SODs that convert superoxide radicals to hydrogen peroxide. Iron is known to be present in catalase that converts peroxide into water and oxygen. Thus metal seems to play a very important role in host-pathogen interactions. We hypothesized that the SODs and catalases could be pumped into the phagolysosome by the bacillus through the *Sec* system. The unfolded enzymes would then refold using metals that are available in the surrounding region. We also think that the 12 P-type ATPases in Mtb are responsible for the transfer of the metal component of these enzymes. To elucidate the substrate for the ctp proteins in Mtb, we have used various bioinformatic approaches to identify the transmembrane metal binding sites and the metal coordinating residues. We have also tried to classify them into the different subgroups in the P-type ATPase family.

Substrate specificity determines the role of the P-type ATPases in the cell. Previous studies

involving P-type ATPases have shown that the region before the cytoplasmic loop containing the DKTGT sequence has conserved amino acids that determine its subtype and metal specificity. Bioinformatic analysis indicates that the ATPases of subgroups P_1, P_{1B}, P_2, and P_3 are present in Mtb. In addition to these P_{1B5} was identified in other Mycobacteria other than Mtb.

Genome wide transposon mutagenesis studies indicate three Ctps important for virulence. i.e. ctpC, G and F [99] [95]. Genomic organization also supports the hypothesis that some of these proteins may also be involved in host pathogen interactions. A possible function can be deduced for these ATPases using the conserved residues that were identified in the TM helices after sequence alignment. It can be deduced that Mtb has at least three copper transporting ATPases; ctpA, B ad V. However copper chaperones were not identified in the search conducted. Analysis of the N and C terminal domains did not show proof of metal binding domains, for regulatory interactions with the protein. ctpC looks like a copper ATPase in all its helices except for H8 where it looks like a mutated copper transporter, with the methionine residue replaced with a histidine. ctpG resembles the rare P-type ATPase previously classified as the P_{1B6} subgroup. Previously no proteins from *Mycobacteria* were found in P_{1B5} subgroup. However there are some proteins from this genus (other than Mtb) that were found to belong to the P_{1B5} subgroup. ctps E, F, H and I belong to the P_2 ATPases. They have to yet be classified into subgroups. Purified proteins have to be analyzed to understand their actual substrate specificity, however we did *E. coli* based assays to determine their putative role. Our results with the *E. coli* showed that the possible substrate could either be Copper or Cadmium. However pNPP analysis done on pure protein showed that the cobalt and manganese inhibited the assay, suggesting that these metals could possibly activate their ATPase activity. Activation of pNPP assay by Cu^+ and Zinc could not be explained by the assay used.

ctpC could be present on the surface of Mtb to efflux metals like Co or Cu that could be useful to act as metal co-factors in the SODs. This could help Mtb to survive better in the toxic environment of the phagolysosome. Data obtained from growth curves suggest that Copper and Cobalt as possible substrates for CtpC. A more conclusive ATPase assay must be performed to elucidate the true nature of the heavy metal substrate for this transporter. These experiments thus provide clues of the possible substrate for ctpC.

5. REFERENCES

1. Dye, C. (2000) Tuberculosis 2000-2010: control, but not elimination. *Int J Tuberc Lung Dis* **4:** S146-52.
2. Clark-Curtiss, J. E. & Haydel, S. E. (2003) Molecular genetics of Mycobacterium tuberculosis pathogenesis. *Annu Rev Microbiol* **57:** 517-549.
3. Clemens, D. L., Lee, B. Y. & Horwitz, M. A. (1995) Purification, characterization, and genetic analysis of Mycobacterium tuberculosis urease, a potentially critical determinant of host-pathogen interaction. *J Bacteriol* **177:** 5644-5652.
4. Frehel, C., Offredo, C. & de Chastellier, C. (1997) The phagosomal environment protects virulent Mycobacterium avium from killing and destruction by clarithromycin. *Infect Immun* **65:** 2792-2802.
5. Zhang, Y., Lathigra, R., Garbe, T., Catty, D. & Young, D. (1991) Genetic analysis of superoxide dismutase, the 23 kilodalton antigen of Mycobacterium tuberculosis. *Mol Microbiol* **5:** 381-391.
6. Harth, G., Clemens, D. L. & Horwitz, M. A. (1994) Glutamine synthetase of Mycobacterium tuberculosis: extracellular release and characterization of its enzymatic activity. *Proc Natl Acad Sci U S A* **91:** 9342-9346.
7. Sonnenberg, M. G. & Belisle, J. T. (1997) Definition of Mycobacterium tuberculosis culture filtrate proteins by two-dimensional polyacrylamide gel electrophoresis, N-terminal amino acid sequencing, and electrospray mass spectrometry. *Infect Immun* **65:** 4515-4524.
8. Sorensen, A. L., Nagai, S., Houen, G., Andersen, P. & Andersen, A. B. (1995) Purification and characterization of a low-molecular-mass T-cell antigen secreted by Mycobacterium tuberculosis. *Infect Immun* **63:** 1710-1717.
9. Nathan, C. & Shiloh, M. U. (2000) Reactive oxygen and nitrogen intermediates in the relationship between mammalian hosts and microbial pathogens. *Proc Natl Acad Sci U S A* **97:** 8841-8848.
10. Ischiropoulos, H. et al. (1992) Peroxynitrite-mediated tyrosine nitration catalyzed by superoxide dismutase. *Arch Biochem Biophys* **298:** 431-437.
11. Zingarelli, B., O'Connor, M., Wong, H., Salzman, A. L. & Szabo, C. (1996) Peroxynitrite-mediated DNA strand breakage activates poly-adenosine diphosphate ribosyl synthetase

and causes cellular energy depletion in macrophages stimulated with bacterial lipopolysaccharide. *J Immunol* **156:** 350-358.

12. Xia, Y. & Zweier, J. L. (1997) Superoxide and peroxynitrite generation from inducible nitric oxide synthase in macrophages. *Proc Natl Acad Sci U S A* **94:** 6954-6958.
13. McCann, J. R., McDonough, J. A., Pavelka, M. S. & Braunstein, M. (2007) Beta-lactamase can function as a reporter of bacterial protein export during Mycobacterium tuberculosis infection of host cells. *Microbiology* **153:** 3350-3359.
14. McDonough, J. A., Hacker, K. E., Flores, A. R., Pavelka, M. S. J. & Braunstein, M. (2005) The twin-arginine translocation pathway of Mycobacterium smegmatis is functional and required for the export of mycobacterial beta-lactamases. *J Bacteriol* **187:** 7667-7679.
15. Finlay, B. B. & Falkow, S. (1997) Common themes in microbial pathogenicity revisited. *Microbiol Mol Biol Rev* **61:** 136-169.
16. Braunstein, M., Espinosa, B. J., Chan, J., Belisle, J. T. & Jacobs, W. R. J. (2003) SecA2 functions in the secretion of superoxide dismutase A and in the virulence of Mycobacterium tuberculosis. *Mol Microbiol* **48:** 453-464.
17. Davis, A. V. & O'Halloran, T. V. (2008) A place for thioether chemistry in cellular copper ion recognition and trafficking. *Nat Chem Biol* **4:** 148-151.
18. O'Halloran, T. V. & Culotta, V. C. (2000) Metallochaperones, an intracellular shuttle service for metal ions. *J Biol Chem* **275:** 25057-25060.
19. Bagai, I., Liu, W., Rensing, C., Blackburn, N. J. & McEvoy, M. M. (2007) Substrate-linked conformational change in the periplasmic component of a Cu(I)/Ag(I) efflux system. *J Biol Chem* **282:** 35695-35702.
20. Culotta, V. C., Yang, M. & O'Halloran, T. V. (2006) Activation of superoxide dismutases: putting the metal to the pedal. *Biochim Biophys Acta* **1763:** 747-758.
21. Agranoff, D. & Krishna, S. (2004) Metal ion transport and regulation in Mycobacterium tuberculosis. *Front Biosci* **9:** 2996-3006.
22. Cole, S. T. et al. (1998) Deciphering the biology of Mycobacterium tuberculosis from the complete genome sequence. *Nature* **393:** 537-544.
23. Argüello, J. M., Mandal, A. K. & Mana-Capelli, S. (2003) Heavy metal transport CPx-ATPases from the thermophile Archaeoglobus fulgidus. *Ann N Y Acad Sci* **986:** 212-218.

24. Axelsen, K. B. & Palmgren, M. G. (1998) Evolution of substrate specificities in the P-type ATPase superfamily. *J Mol Evol* **46:** 84-101.
25. Axelsen, K. B. & Palmgren, M. G. (2001) Inventory of the superfamily of P-type ion pumps in Arabidopsis. *Plant Physiol* **126:** 696-706.
26. Bull, P. C. & Cox, D. W. (1994) Wilson disease and Menkes disease: new handles on heavy-metal transport. *Trends Genet.* **10:** 246-252.
27. Lutsenko, S. & Kaplan, J. H. (1995) Organization of P-type ATPases: significance of structural diversity. *Biochemistry* **34:** 15607-15613.
28. Solioz, M. & Vulpe, C. (1996) CPx-type ATPases: a class of P-type ATPases that pump heavy metals. *Trends Biochem. Sci.* **21:** 237-241.
29. Argüello, J. M. (2003) Identification of ion-selectivity determinants in heavy-metal transport P1B-type ATPases. *J Membr Biol* **195:** 93-108.
30. Mandal, A. K., Yang, Y., Kertesz, T. M. & Argüello, J. M. (2004) Identification of the transmembrane metal binding site in Cu+-transporting PIB-type ATPases. *J Biol Chem* **279:** 54802-54807.
31. Sazinsky, M. H., Mandal, A. K., Argüello, J. M. & Rosenzweig, A. C. (2006) Structure of the ATP binding domain from the Archaeoglobus fulgidus Cu+-ATPase. *J Biol Chem* **281:** 11161-11166.
32. Sazinsky, M. H., Agarwal, S., Argüello, J. M. & Rosenzweig, A. C. (2006) Structure of the actuator domain from the *Archaeoglobus fulgidus* Cu(+)-ATPase. *Biochemistry* **45:** 9949-9955.
33. Banci, L. et al. (2005) An atomic-level investigation of the disease-causing A629P mutant of the Menkes protein, ATP7A. *J. Mol. Biol.* **352:** 409-417.
34. Post, R. L., Hegyvary, C. & Kume, S. (1972) Activation by adenosine triphosphate in the phosphorylation kinetics of sodium and potassium ion transport adenosine triphosphatase. *J Biol Chem* **247:** 6530-6540.
35. Eren, E. & Argüello, J. M. (2004) Arabidopsis HMA2, a divalent heavy metal-transporting P(IB)-type ATPase, is involved in cytoplasmic Zn2+ homeostasis. *Plant Physiol* **136:** 3712-3723.
36. Fan, B. & Rosen, B. P. (2002) Biochemical characterization of CopA, the *Escherichia coli* Cu(I)-translocating P-type ATPase. *J Biol Chem* **277:** 46987-46992.

37. Mana-Capelli, S., Mandal, A. K. & Argüello, J. M. (2003) *Archaeoglobus fulgidus* CopB is a thermophilic Cu2+-ATPase: functional role of its histidine-rich-N-terminal metal binding domain. *J Biol Chem* **278:** 40534-40541.
38. Sharma, R., Rensing, C., Rosen, B. P. & Mitra, B. (2000) The ATP hydrolytic activity of purified ZntA, a Pb(II)/Cd(II)/Zn(II)-translocating ATPase from Escherichia coli. *J Biol Chem* **275:** 3873-3878.
39. Tsivkovskii, R., Eisses, J. F., Kaplan, J. H. & Lutsenko, S. (2002) Functional properties of the copper-transporting ATPase ATP7B (the Wilson's disease protein) expressed in insect cells. *J Biol Chem* **277:** 976-983.
40. Voskoboinik, I., Brooks, H., Smith, S., Shen, P. & Camakaris, J. (1998) ATP-dependent copper transport by the Menkes protein in membrane vesicles isolated from cultured Chinese hamster ovary cells. *FEBS Letters* **435:** 178-182.
41. Rensing, C., Mitra, B. & Rosen, B. P. (1997) The zntA gene of Escherichia coli encodes a Zn(II)-translocating P-type ATPase. *Proc Natl Acad Sci U S A* **94:** 14326-14331.
42. Odermatt, A., Suter, H., Krapf, R. & Solioz, M. (1993) Primary structure of two P-type ATPases involved in copper homeostasis in Enterococcus hirae. *J Biol Chem* **268:** 12775-12779.
43. Tottey, S., Rich, P. R., Rondet, S. A. & Robinson, N. J. (2001) Two Menkes-type atpases supply copper for photosynthesis in Synechocystis PCC 6803. *J Biol Chem* **276:** 19999-20004.
44. Kaplan, J. H. (2002) Biochemistry of Na,K-ATPase. *Annu Rev Biochem* **71:** 511-535.
45. Toyoshima, C. & Inesi, G. (2004) Structural basis of ion pumping by Ca2+-ATPase of the sarcoplasmic reticulum. *Annu Rev Biochem* **73:** 269-292.
46. Rensing, C., Ghosh, M. & Rosen, B. P. (1999) Families of soft-metal-ion-transporting ATPases. *J. Bacteriol* **181:** 5891-5897.
47. Lowe, J. et al. (2004) A mutational study in the transmembrane domain of Ccc2p, the yeast Cu(I)-ATPase, shows different roles for each Cys-Pro-Cys cysteine. *J. Biol. Chem.* **279:** 25986-25994.
48. Mandal, A. K., Mikhailova, L. & Argüello, J. M. (2003) The Na,K-ATPase S5-H5 helix: structural link between phosphorylation and cation-binding sites. *Ann N Y Acad Sci* **986:** 224-225.

49. Yoshimizu, T., Omote, H., Wakabayashi, T., Sambongi, Y. & Futai, M. (1998) Essential Cys-Pro-Cys motif of *Caenorhabditis elegans* copper transport ATPase. *Biosci Biotechnol Biochem.* **62:** 1258-1260.
50. Arguello, J. M. & Kaplan, J. H. (1994) Glutamate 779, an intramembrane carboxyl, is essential for monovalent cation binding by the Na,K-ATPase. *J Biol Chem* **269:** 6892-6899.
51. Arguello, J. M. & Lingrel, J. B. (1995) Substitutions of serine 775 in the alpha subunit of the Na,K-ATPase selectively disrupt K+ high affinity activation without affecting Na+ interaction. *J Biol Chem* **270:** 22764-22771.
52. Arguello, J. M., Peluffo, R. D., Feng, J., Lingrel, J. B. & Berlin, J. R. (1996) Substitution of glutamic 779 with alanine in the Na,K-ATPase alpha subunit removes voltage dependence of ion transport. *J Biol Chem* **271:** 24610-24616.
53. MacLennan, D. H., Rice, W. J. & Green, N. M. (1997) The mechanism of Ca^{2+} transport by sarco(endo)plasmic reticulum Ca2+-ATPases. *J Biol Chem* **272:** 28815-28818.
54. Vilsen, B. & Andersen, J. P. (1992) CrATP-induced Ca^{+2} occlusion in mutants of the Ca(2+)-ATPase of sarcoplasmic reticulum. *J. Biol. Chem.* **26:** 25739-25743.
55. Toyoshima, C., Nakasako, M., Nomura, H. & Ogawa, H. (2000) Crystal structure of the calcium pump of sarcoplasmic reticulum at 2.6 A resolution. *Nature* **405:** 647-655.
56. Dunbar, L. A. et al. (1997) Sorting of ion pumps in polarized epithelial cells. *Ann N Y Acad Sci* **834:** 514-523.
57. Argüello, J. M., Eren, E. & González-Guerrero, M. (2007) The structure and function of heavy metal transport P(1B)-ATPases. *Biometals* **20:** 233-248.
58. Arnesano, F. et al. (2002) Metallochaperones and metal-transporting ATPases: A comparative analysis of sequences and structures. *Gen. Res.* **12:** 255-271.
59. Lutsenko, S. & Petris, M. J. (2003) Function and regulation of the mammalian copper-transporting ATPases: insights from biochemical and cell biological approaches. *J Membr Biol* **191:** 1-12.
60. Bal, N., Wu, C. C., Catty, P., Guillain, F. & Mintz, E. (2003) Cd2+ and the N-terminal metal-binding domain protect the putative membranous CPC motif of the Cd2+-ATPase of Listeria monocytogenes. *Biochem J* **369:** 681-685.

61. Fan, B. & Rosen, B. P. (2002) Biochemical characterization of CopA, the Escherichia coli Cu(I)-translocating P-type ATPase. *J Biol Chem* **277:** 46987-46992.
62. Mandal, A. K. & Argüello, J. M. (2003) Functional roles of metal binding domains of the Archaeoglobus fulgidus Cu(+)-ATPase CopA. *Biochemistry* **42:** 11040-11047.
63. Mitra, B. & Sharma, R. (2001) The cysteine-rich amino-terminal domain of ZntA, a Pb(II)/Zn(II)/Cd(II)-translocating ATPase from Escherichia coli, is not essential for its function. *Biochemistry* **40:** 7694-7699.
64. Voskoboinik, I., Greenough, M., La Fontaine, S., Mercer, J. F. B. & Camakaris, J. (2001) Functional studies on the Wilson copper P-type ATPase and toxic milk mouse mutant. *Biochemical and Biophysical Research Communications* **281:** 966-970.
65. Voskoboinik, I. et al. (1999) Functional analysis of the N-terminal CXXC metal-binding motifs in the human Menkes copper-transporting P-type ATPase expressed in cultured mammalian cells. *J. Biol. Chem.* **274:** 22008-22012.
66. Eren, E., Gonzalez-Guerrero, M., Kaufman, B. M. & Arguello, J. M. (2007) Novel Zn2+ coordination by the regulatory N-terminus metal binding domain of Arabidopsis thaliana Zn(2+)-ATPase HMA2. *Biochemistry* **46:** 7754-7764.
67. Eren, E., Kennedy, D. C., Maroney, M. J. & Argüello, J. M. (2006) A novel regulatory metal binding domain is present in the C terminus of Arabidopsis Zn2+-ATPase HMA2. *J Biol Chem* **281:** 33881-33891.
68. Altschul, S. F., Gertz, E. M., Agarwala, R., Schaffer, A. A. & Yu, Y. K. (2009) PSI-BLAST pseudocounts and the minimum description length principle. *Nucleic Acids Res* **37:** 815-824.
69. Gasteiger, E. et al. (2003) ExPASy: The proteomics server for in-depth protein knowledge and analysis. *Nucleic Acids Res* **31:** 3784-3788.
70. Hirokawa, T., Boon-Chieng, S. & Mitaku, S. (1998) SOSUI: classification and secondary structure prediction system for membrane proteins. *Bioinformatics* **14:** 378-379.
71. K, H. & W, S. (1993) A Database of Membrane Spanning Protein Segments. *Biol. Chem. Hoppe-Seyler* **374:** 166.
72. Tusnady, G. E. & Simon, I. (2001) The HMMTOP transmembrane topology prediction server. *Bioinformatics* **17:** 849-850.

73. Cserzo, M., Wallin, E., Simon, I., von Heijne, G. & Elofsson, A. (1997) Prediction of transmembrane alpha-helices in prokaryotic membrane proteins: the dense alignment surface method. *Protein Eng* **10:** 673-676.
74. Rost, B., Yachdav, G. & Liu, J. (2004) The PredictProtein server. *Nucleic Acids Res* **32:** W321-6.
75. Bradford, M. M. (1976) A rapid and sensitive method for the quantification of microgram quantities of protein utilizing the principle of protein-dye binding. *Anal. Biochem.* **72:** 248-254.
76. Outten, C. E. & O'Halloran, T. V. (2001) Femtomolar sensitivity of metalloregulatory proteins controlling zinc homeostasis. *Science* **292:** 2488-2492.
77. Mandal, A. K., Cheung, W. D. & Argüello, J. M. (2002) Characterization of a thermophilic P-type Ag+/Cu+-ATPase from the extremophile Archaeoglobus fulgidus. *J Biol Chem* **277:** 7201-7208.
78. Laemmli, U. K. (1970) Cleaveage of structural proteins during the assembly of the head of bacteriophage T4. *Nature* **227:** 680-685.
79. Yang, Y., Mandal, A. K., Bredestón, L. M., Luis González-Flecha, F. & Argüello, J. M. (2007) Activation of *Archaeoglobus fulgidus* Cu(+)-ATPase CopA by cysteine. *Biochim Biophys Acta* **1768:** 495-501.
80. Bull, P. C., Thomas, G. R., Rommens, J. M., Forbes, J. R. & Cox, D. W. (1993) The Wilson disease gene is a putative copper transporting P-type ATPase similar to the Menkes gene. *Nat Genet* **5:** 327-337.
81. Petrukhin, K. & Gilliam, T. C. (1994) Genetic disorders of copper metabolism. *Curr Opin Pediatr* **6:** 698-701.
82. Petrukhin, K. et al. (1994) Characterization of the Wilson disease gene encoding a P-type copper transporting ATPase: genomic organization, alternative splicing, and structure/function predictions. *Hum Mol Genet* **3:** 1647-1656.
83. Hirayama, T. et al. (1999) RESPONSIVE-TO-ANTAGONIST1, a Menkes/Wilson disease-related copper transporter, is required for ethylene signaling in Arabidopsis. *Cell* **97:** 383-393.

84. Woeste, K. E. & Kieber, J. J. (2000) A strong loss-of-function mutation in RAN1 results in constitutive activation of the ethylene response pathway as well as a rosette-lethal phenotype. *Plant Cell* **12:** 443-455.
85. Rensing, C., Fan, B., Sharma, R., Mitra, B. & Rosen, B. P. (2000) CopA: An Escherichia coli Cu(I)-translocating P-type ATPase. *Proceedings of the National Academy of Sciences of the United States of America* **97:** 652-656.
86. Bramkamp, M., Altendorf, K. & Greie, J. C. (2007) Common patterns and unique features of P-type ATPases: a comparative view on the KdpFABC complex from Escherichia coli (Review). *Mol Membr Biol* **24:** 375-386.
87. Schwan, W. R., Warrener, P., Keunz, E., Stover, C. K. & Folger, K. R. (2005) Mutations in the cueA gene encoding a copper homeostasis P-type ATPase reduce the pathogenicity of Pseudomonas aeruginosa in mice. *Int J Med Microbiol* **295:** 237-242.
88. Francis, M. S. & Thomas, C. J. (1996) Effect of multiplicity of infection on Listeria monocytogenes pathogenicity for HeLa and Caco-2 cell lines. *J Med Microbiol* **45:** 323-330.
89. Gonzalez-Guerrero, M., Eren, E., Rawat, S., Stemmler, T. L. & Arguello, J. M. (2008) Structure of the two transmembrane Cu+ transport sites of the Cu+ -ATPases. *J Biol Chem* **283:** 29753-29759.
90. Rutherford, J. C., Cavet, J. S. & Robinson, N. J. (1999) Cobalt-dependent transcriptional switching by a dual-effector MerR-like protein regulates a cobalt-exporting variant CPx-type ATPase. *J Biol Chem* **274:** 25827-25832.
91. Seigneurin-Berny, D. et al. (2006) HMA1, a new Cu-ATPase of the chloroplast envelope, is essential for growth under adverse light conditions. *J Biol Chem* **281:** 2882-2892.
92. Moreno, I. et al. (2008) AtHMA1 is a thapsigargin-sensitive Ca2+/heavy metal pump. *J Biol Chem* **283:** 9633-9641.
93. Arguello, J. M., Eren, E. & Gonzalez-Guerrero, M. (2007) The structure and function of heavy metal transport P1B-ATPases. *Biometals* **20:** 233-248.
94. Lingrel, J. B., Croyle, M. L., Woo, A. L. & Arguello, J. M. (1998) Ligand binding sites of Na,K-ATPase. *Acta Physiol Scand Suppl* **643:** 69-77.
95. Sassetti, C. M. & Rubin, E. J. (2003) Genetic requirements for mycobacterial survival during infection. *Proc Natl Acad Sci U S A* **100:** 12989-12994.

96. Sassetti, C. M., Boyd, D. H. & Rubin, E. J. (2001) Comprehensive identification of conditionally essential genes in mycobacteria. *Proc Natl Acad Sci U S A* **98:** 12712-12717.
97. Rengarajan, J., Bloom, B. R. & Rubin, E. J. (2005) Genome-wide requirements for Mycobacterium tuberculosis adaptation and survival in macrophages. *Proc Natl Acad Sci U S A* **102:** 8327-8332.
98. Rao, S. P. et al. (2008) Recombinase-based reporter system and antisense technology to study gene expression and essentiality in hypoxic nonreplicating mycobacteria. *FEMS Microbiol Lett* **284:** 68-75.
99. Sassetti, C. M., Boyd, D. H. & Rubin, E. J. (2003) Genes required for mycobacterial growth defined by high density mutagenesis. *Mol Microbiol* **48:** 77-84.